Auxiliary Material Submission for Paper 2005JBXXXXXX

Spatio-temporal evolution of a transient slip event on the San Andreas Fault near Parkfield, California

Jessica Murray (U.S. Geological Survey, Menlo Park, CA) and Paul Segall (Stanford University)

PAPER REFERENCE

Introduction

The auxiliary material contains an extended discussion of the creepmeter observations that were used as constraints in the time-dependent analysis of the two-color EDM data, as well as a figure showing the creep time series used in our analyses.

1) PAPERNUMBER-CREEP.txt The discussion of creepmeter observations.

2) PAPPERNUMBER-figureS1.eps (figure S1) Creep meter time series. Solid lines are the time series with seasonal noise removed. Dashed lines, in addition to removal of the seasonal noise, have been smoothed along strike and, for creepmeters xmm1, xmd1, xva1, and xpk1, have an added secular trend. Roeloffs [2001] found that the accelerated creep at wrk1 in 1995 may be rainfall-induced. She also noted that the apparent instability of x461 is likely due to its location on a slope, as well as the influence of rainfall and anthropogenic noise sources. In our analysis, the creep at x461 was taken to be zero during the time it showed left-lateral motion. Finally, Roeloffs [2001] attributed the low creep rate at xmd1 to the combined influence of two factors: 1) the instrument does not span the entire fault zone and 2) it experiences rainfall-induced left lateral creep.

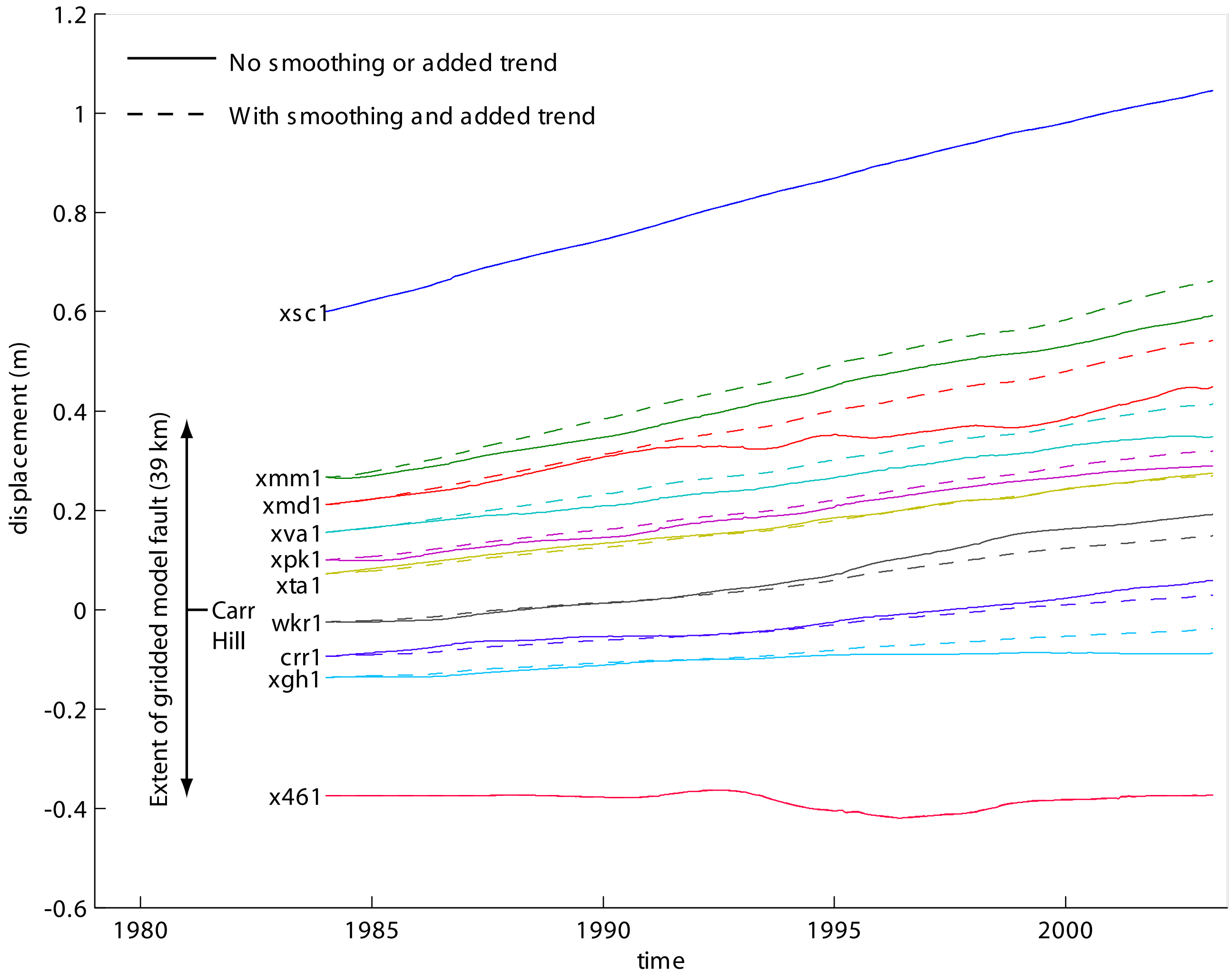
No smoothing or added trend
With smoothing and added trend
displacement (m)
time
1.2
1
0.8
0.6
0.4
0.2
0
-0.2
-0.4
-0.6
1980
1985
1990
1995
2000
xsc1
xmm1
xmd1
xva1
xpk1
xta1
wkr1
crr1
xgh1
x461
Extent of gridded model fault (39 km)
Carr Hill

The creepmeter data were used to provide constraints on the surface-breaking subfaults as follows. For each creepmeter, the data were decimated to daily observations by taking the mean of each day's measurements. Before conducting the time-dependent inversion for fault slip, we used the ENIF to estimate and remove the seasonal noise from the creep time series (figure S1). In order to obtain a time series for each surface-breaking subfault, we used linear interpolation between creepmeters to fill along-strike gaps in coverage (e.g., at the southeast end of the model fault). In the time dependent analysis of the two-color data, creep observations were used only on days for which there were two-color data.

To address potential sources of bias in the creep time series (e.g., those discussed by Roeloffs [2001]), we also conducted a time-dependent inversion of the two-color data using two additional steps in obtaining the constraints. First, to mitigate the effects of large localized variations in creep behavior between neighboring sites, we smoothed the time series along strike using a second difference operator. Second, we added a linear trend to the creep time series of four sites northwest of Carr Hill (xmm1, xmd1, xva1, and xpk1) that may not span the whole fault zone [Roeloffs, 2001] so that their long-term rates approximated those obtained from alinement arrays and small aperture geodetic networks [Lisowski and Prescott, 1981]. The resulting time series (figure S1), which were used in the results presented in the paper, had long-term average rates decreasing from ~24 mm/yr in the NW to ~3 mm/yr in the SE.

The results of the time-dependent inversion of the two-color data were essentially the same regardless of which of the two sets of surface constraints we used, and the subtle differences between the two solutions do not alter the conclusions of our paper.